High Mobility Field-Effect Transistors with Versatile Processing from a Small-Molecule Organic Semiconductor

Yaochuan Mei, Marsha A. Loth, Marcia Payne, Weimin Zhang, Jeremy Smith, Cynthia S. Day, Sean R. Parkin, Martin Heeney, Iain McCulloch, Thomas D. Anthopoulos, John E. Anthony, and Oana D. Jurchescu**

Along with excellent potential for commercial applications such as displays or sensors,[1] organic semiconductors offer a versatile platform to understand the fundamental structural and process parameters governing charge transport in carbon-based solids. In earlier work, we demonstrated how the addition of specific functional groups to the anthradithiophene chromophore allowed tuning of the solid-state order of these now soluble materials to enhance hole mobility in thin-film transistors.[2] We later found that the addition of two fluorine substituents both enhanced the stability of the organic material and subtly changed the crystal packing to further enhance charge transport.[3–5] We report here a further modification–replacing the trialkylsilyl substituent with its trialkygermyl homolog–that again subtly changes the solid-state order and yields a significant improvement in performance, along with permitting processing by an array of methods suitable for large-area deposition.

The triethylgermylethynyl-substituted anthradithiophene (diF-TEG ADT, **Figure 1** a) is easily prepared as an inseparable mixture of *syn* and *anti* isomers by standard chemical synthesis. We have shown in previous studies that the presence of the two isomers does not significantly impact device performance.[6] The molecular structure and representation of the molecular packing, emphasizing the two-dimensional π-stacked arrangement, are shown in Figure 1. The molecules adopt a 2D π-stacking motif (Figure 1b), similar to triethylsilylethynyl-substituted anthradithiophene - diF-TES ADT, with the slight increase in C-Ge bond length compared with the C-Si bond allowing closer interplanar spacing (3.24 Å in diF-TEG ADT compared to 3.37 Å in diF-TES ADT).[5] We also observe other subtle differences between the crystal packing of the diF-TES ADT and diF-TEG ADT compounds, such as a 1.8 Å smaller shift along the long-axis between adjacent molecules, and 11% larger areal molecular overlap for the TEG compound. These variations in molecular arrangement suggest improvement in charge transport properties, as predicted by theoretical studies showing that such differences can strongly affect the intermolecular electronic couplings.[7] XRD measurements performed on thin films deposited from a chlorobenzene solution on an Au surface treated with pentafluorobenzene thiol (PFBT) self-assembly monolayer indicate that the diF-TEG ADT films exhibit a high degree of crystallinity, with the molecules adopting a preferred orientation along the (001) direction (Figure 1c). This orientation, with the molecular backbones aligned "edge-on" (approximately perpendicular to the surface) and the *ab* plane parallel to the substrate (Figure 1d) yields π-π overlap in the plane of the substrate, which is believed critical for high charge carrier mobilities.[8,9]

To explore the transport properties and processing possibilities of this new material, field-effect transistors (FETs) were fabricated by a number of methods. Bottom contact, bottom gate FETs with configuration similar to the one presented in **Figure 2**a were fabricated on substrates consisting of highly doped silicon (the gate electrode), and thermally grown SiO_2 as gate dielectric. Source and drain Au contacts were defined photolithographically with channel lengths between 5 and 100 m. The contacts were chemically treated with PFBT prior to film deposition to improve crystallization and charge injection.[8] Initially, the organic semiconductor was deposited on these substrates using drop-casting in a solvent-rich atmosphere (SAC - solvent assisted crystallization).[10] The optical micrograph and electrical properties of a representative device obtained by SAC are depicted in Figure 2b, c and d respectively. The crystallites forming the films are red, platelet-like (Figure 2b). The evolution of the drain current (I_D) with the source-drain voltage (V_{DS}) for several source-gate (V_{GS}) voltages plotted in Figure 2c indicates that hole transport is characteristic for this

Y. Mei,[+] Prof. O. D. Jurchescu
Department of Physics
Wake Forest University
Winston-Salem, NC 27109 USA
E-mail: jurchescu@wfu.edu
Dr. C. S. Day
Department of Chemistry
Wake Forest University
Winston-Salem, NC 27109 USA
Dr. W. Zhang, Prof. M. Heeney, Prof. I. McCulloch
Department of Chemistry and Centre for Plastic Electronics
Imperial College London, SW7 2AZ UK
Dr. J. Smith, Prof. T. D. Anthopoulos
Department of Physics and Centre for Plastic Electronics
Blackett Laboratory, Imperial College London
London SW7 2AZ UK
M. A. Loth,[+] Dr. M. Payne, Dr. S. R. Parkin, Prof. J. E. Anthony
Department of Chemistry, University of Kentucky
Lexington, KY 40506 USA
Email: anthony@uky.edu
[+] These authors contributed equally to this work.

DOI: 10.1002/adma.201205371

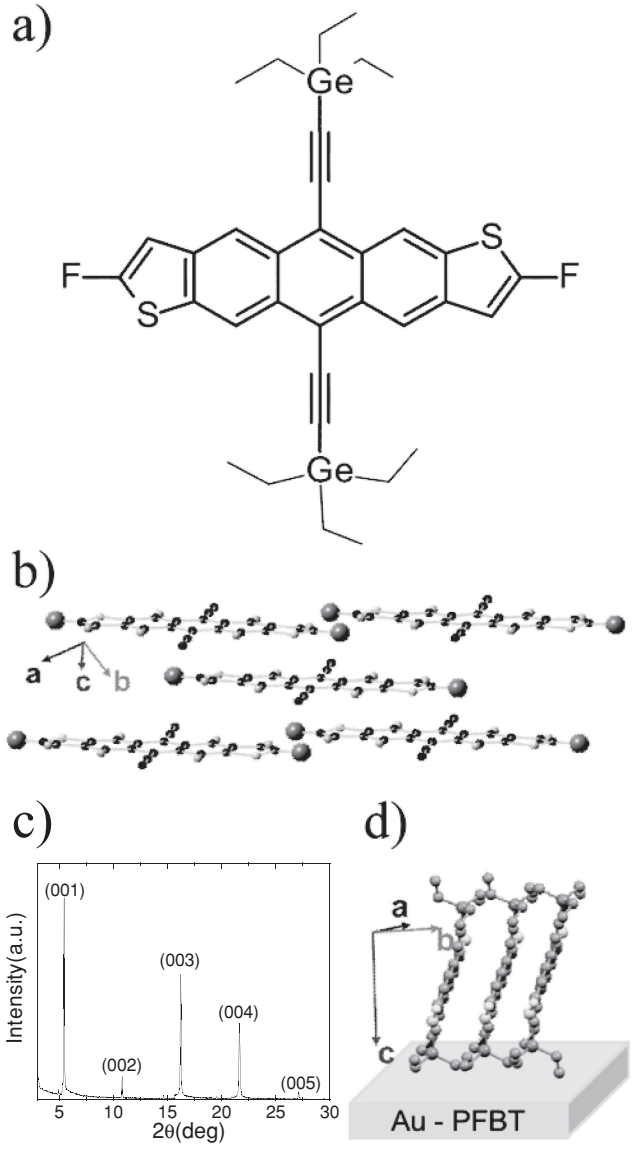

Figure 1. a) Molecular structure of diF-TEG ADT. b) Crystalline order showing 2D-bricklayer arrangement of the molecules in the crystal with significant face-to-face interactions. c) θ–2θ XRD results for a diF-TEG ADT film on a PFBT treated gold substrate, showing the preferential orientation with respect to the surface. d) Molecular orientation on the PFBT/Au surface.

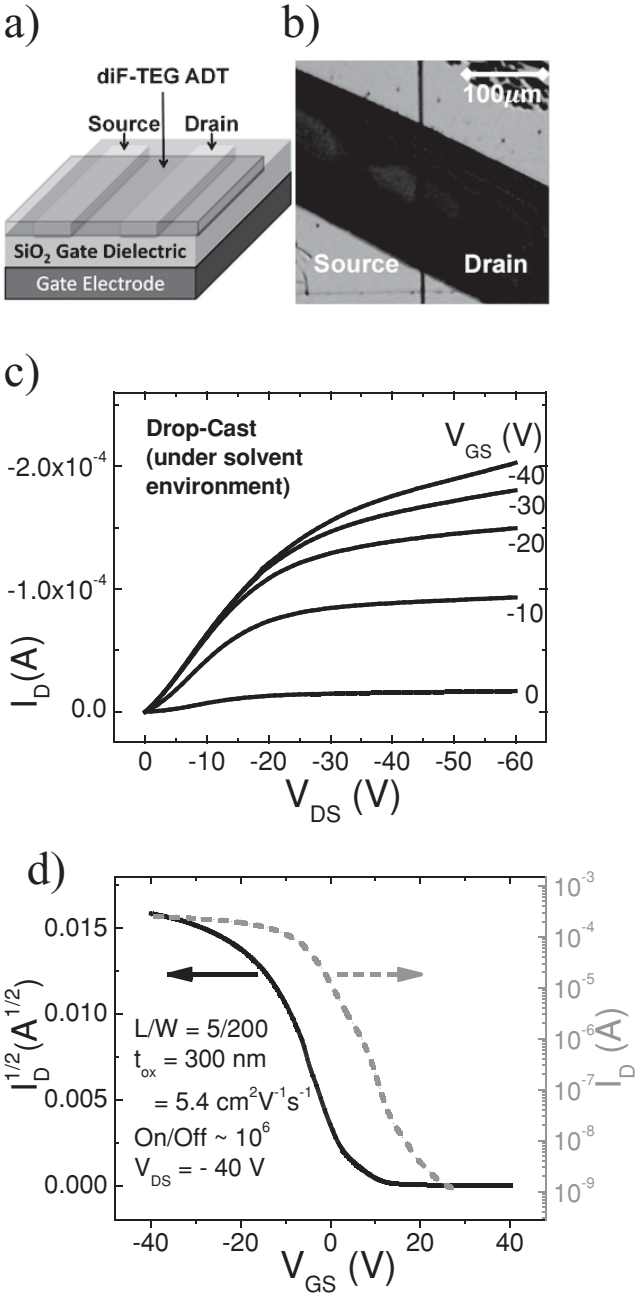

Figure 2. diF-TEG ADT field-effect transistors. a) Device structure, with bottom gate consisting of SiO_2 dielectric and bottom Au source-drain contacts. b) Photo of a device (top view). c) Output characteristics for a device with L = 5 m and W = 200 m. d) Transfer characteristics of the same device in the saturation regime (V_{DS} = –40 V). Right axis: ($\log(I_D)$ vs V_{GS}). Left axis: $\sqrt{I_D}$ vs V_{GS}.

material when Au contacts are used. The compression and curvature of I_D in the linear regime of device operation (low V_{DS}) is not uncommon in high-mobility organic thin-film transistors (OTFTs), especially at short channel lengths, and arises from the fact that here the charge injection and collection efficiencies at the contacts are challenged by the high current density generated in the transistor channel.[11] In Figure 2d we plot the evolution of the I_D versus V_{GS} in the saturation regime (V_{DS} = –40V) for the same device, having channel length L = 5 m and channel width W = 200 m. From the curve on the right axis we estimate the on/off ratio to be ~10^6 and from the curve on the left axis, we calculate a field-effect mobility = 5.4 cm^2 V^{-1} s^{-1}. This value is significantly higher than the best mobility reported in solution deposited diF-TES ADT: a summary of the highest reported mobilities in diF-TEG ADT (this work) and diF-TES ADT (references included) is compiled in **Table 1**. The threshold voltage shifts towards positive values when the measurement is performed in ambient conditions, which is qualitatively consistent with an oxidative oxygen

Adv. Mater. 2013,
DOI: 10.1002/adma.201205371

Table 1. Charge carrier mobilities of diF-TES ADT and diF-TEG ADT in devices fabricated by drop-casting (under solvent rich atmosphere), spin-coating and spray-deposition.

Material	$_{Drop\text{-}Cast}$ ($cm^2\ V^{-1}\ s^{-1}$)	$_{Spin}$ ($cm^2\ V^{-1}\ s^{-1}$)	$_{Spray}$ ($cm^2\ V^{-1}\ s^{-1}$)
di-F TES ADT	1.5[3]	0.4[18]	0.2[16]
di-F TEG ADT	5.4	3.7	2.2

doping and is under investigation,[12] but we were able to mitigate these parasitic currents with vacuum outgassing of the sample and performing the FET characterization in vacuum.

The histogram in **Figure 3** reviews the values of the mobility recorded on 104 devices fabricated by SAC. The mean value of the mobility was 2.3 ± 1.1 $cm^2\ V^{-1}\ s^{-1}$, with the lowest recorded value of 0.14 $cm^2\ V^{-1}\ s^{-1}$ and the highest of 5.4 $cm^2\ V^{-1}\ s^{-1}$. Such a spread in mobilities is quite common in organic FETs, including single crystal devices, and can originate from such effects as the quality of the metal/semiconductor and metal/dielectric interfaces, thin-film structure and morphology, contact resistance and anisotropy in electrical properties along different crystallographic directions. Nevertheless, the fact that 94 devices (90% of the total measured) exhibited mobilities greater than 1 $cm^2\ V^{-1}\ s^{-1}$, and the best recorded mobility was as high as 5.4 $cm^2\ V^{-1}\ s^{-1}$, makes diF-TEG ADT one of the highest mobility solution-deposited organic semiconductors reported to date. At the same time, our measurements are influenced by morphological effects that cannot be controlled accurately with solution processing, and which impeded access to intrinsic properties of this material. We are currently pursuing single crystal growth by physical vapor transport to be able to access the ultimate performance of this material.[5]

A recent approach to improve device-to-device performance issues involves blending the small-molecule semiconductor into an insulating or semiconducting polymer.[13] In the case of diF-TES ADT, blends with a poly(triarylamine) led to impressive device performance with excellent reproducibility from spin-cast films.[14] Because of the nature of the phase separation of the two species, best performance is observed in top-gate, bottom-contact devices. Thus, a 1:1 weight ratio blend of diF-TEG ADT and poly(triarylamine) was dissolved in tetralin and spin-cast onto a substrate with pre-patterned PFBT-treated Au source and drain electrodes. The as-spun films were annealed at 100 C for 5 minutes, during which time the small-molecule semiconductor dried forming crystalline domains in the range 10–100 m in diameter (**Figure 4** a,b). CYTOP was next deposited as gate dielectric followed by the evaporation of Al through a shadow mask to form the gate electrode. Although maximum mobility in this configuration was not as high as observed in the SAC-deposited films, device-to-device variability did appear to decrease, with a mobility of 1.28 ± 0.05 $cm^2\ V^{-1}\ s^{-1}$ being recorded.

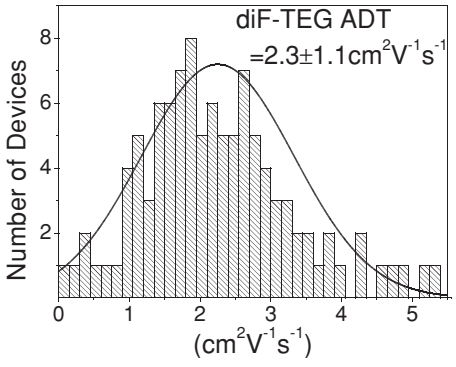

Figure 3. Histogram showing the values of mobilities ( ) measured for 104 diF-TEG ADT devices. The highest mobility is 5.4 $cm^2\ V^{-1}\ s^{-1}$, and the average value is 2.3 ± 1.1 $cm^2\ V^{-1}\ s^{-1}$.

As exemplified by the blend work described above, significant progress has been made recently in device processing, resulting in steady improvements in FET properties. Nevertheless, often these properties can only be reproduced over small areas, when deposition methods such as spin-coating, or drop-casting are used and fail when large-areas are employed. Reproducing the performance obtained with conventional deposition techniques is not trivial given its strong dependence on film morphology and microstructure, which in turn are dictated by processing parameters. Recent reports on spray-deposited FETs have generated interest in this inexpensive, unconventional electronic device manufacturing technique, compatible with arbitrary large-area substrates. For example, Chan et al have measured mobilities of 0.023 $cm^2\ V^{-1}\ s^{-1}$ in polymer FETs based on air-brushed P3HT.[15] We have demonstrated spray-deposited small-molecule FETs with mobilities of 0.2 $cm^2\ V^{-1}\ s^{-1}$ based on diF-TES ADT.[16] Motivated by the remarkable electrical properties of diF-TEG ADT in drop-cast and spin-coated blend devices, we fabricated spray-coated FETs to test the compatibility of this material with methods applicable to large-area electronics. In a bottom-gate, bottom-contact configuration, diF-TEG ADT was deposited by spray deposition of a 0.15 wt% solution in chlorobenzene. Control over the droplet properties was achieved by tuning the pressure of the transporting gas and the distance between the spray nozzle and the substrate. In **Figure 5** we plot the device structure and the current-voltage characteristics of one of the best devices, fabricated under ambient conditions, with the Argon propellant set to a pressure of 5 psi, and with the airbrush positioned perpendicular to the device substrate, at a height of 13 cm. A mobility of = 2.2 $cm^2\ V^{-1}\ s^{-1}$ was calculated from the transfer characteristics in the saturation regime (V_{DS} = −40 V), plotted in Figure 5a. To the best of our knowledge, this value represents the highest mobility reported to date in spray-coated organic FETs. Other characteristics for this device include a very small threshold voltage (V_t = 0.5 V) and a good current on/off ratio (I_{on}/I_{off} ~10^4). An average mobility of 1.1 ± 0.5 $cm^2\ V^{-1}\ s^{-1}$ was determined from measuring 36 devices fabricated under similar conditions (Figure 1, SI).

In summary, the replacement of a trialkylsilyl substituent with a trialkylgermyl group led to subtle but significant changes in molecular packing, which in turn yielded impressive improvements in device performance. Solution-processed OTFTs based on diF-TEG ADT exhibit field-effect mobilities as high as 5.4 $cm^2\ V^{-1}\ s^{-1}$. Devices with a record-high mobility of 2.2 $cm^2\ V^{-1}\ s^{-1}$ are fabricated using spray-deposition, which highlights the promise of this material for incorporation in low-cost, large-area electronics.

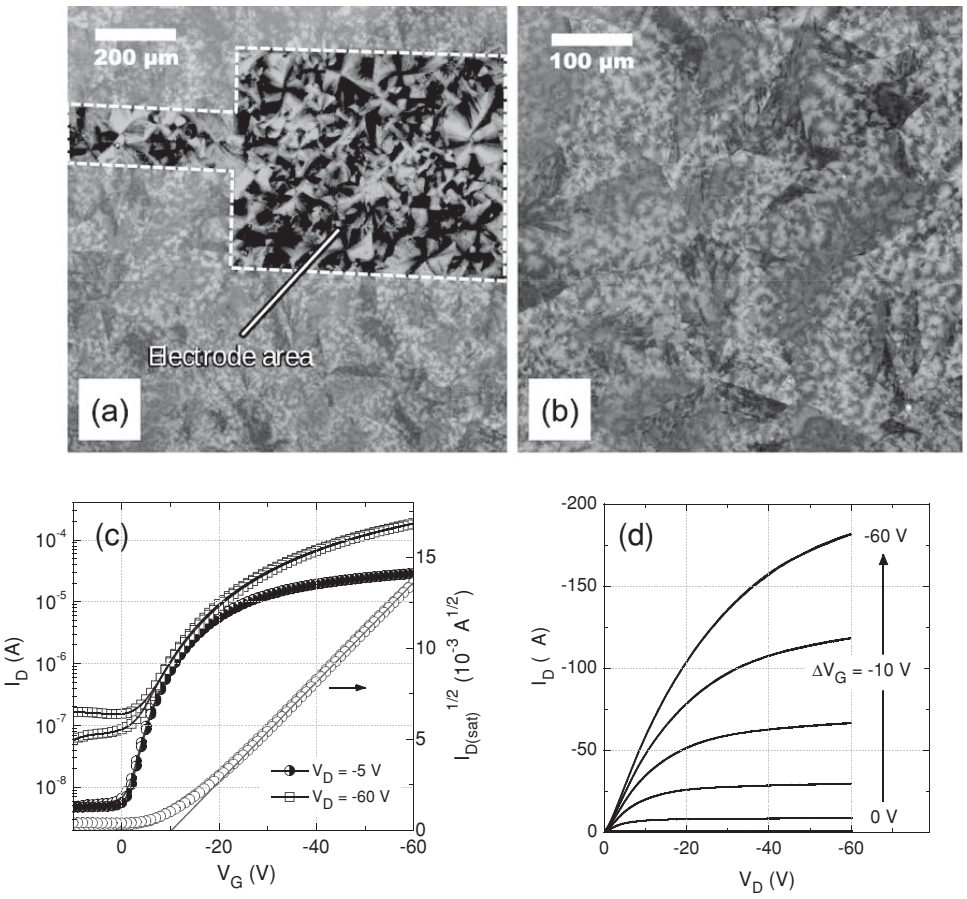

Figure 4. Polarized light microscopy image of a diF-TEG ADT: poly(triarylamine) blend film spin-cast onto glass substrates containing; a Au/PFBT electrode (a–electrode area indicated) and a highest magnification image of the same film onto bare glass area (b). Transfer (c) and output (d) characteristics for transistors fabricated using a 1:1 (by weight) blend of diF-TEG ADT and poly(triarylamine), with channel length and width of L = 20 μm and W = 1000 μm, respectively.

Experimental Section

Material Synthesis: Triethylgermyl acetylene was prepared by adding 200 mL of 0.5 M (100 mmol) ethynyl Grignard in THF solution to a flame dried 500 mL round bottom flask under nitrogen. Triethylchlorogermane (4.87 g, 25 mmol) was added dropwise at room temperature and the solution was stirred overnight at room temperature. After TLC with potassium permanganate stain confirmed completion, the reaction mixture was quenched with water and 10% HCl solution. After extraction with pentane, the organic layer was dried, filtered, and the solvent removed by simple distillation. Silica chromatography with pentane was used to remove a slight brown color and after distillation of the pentane

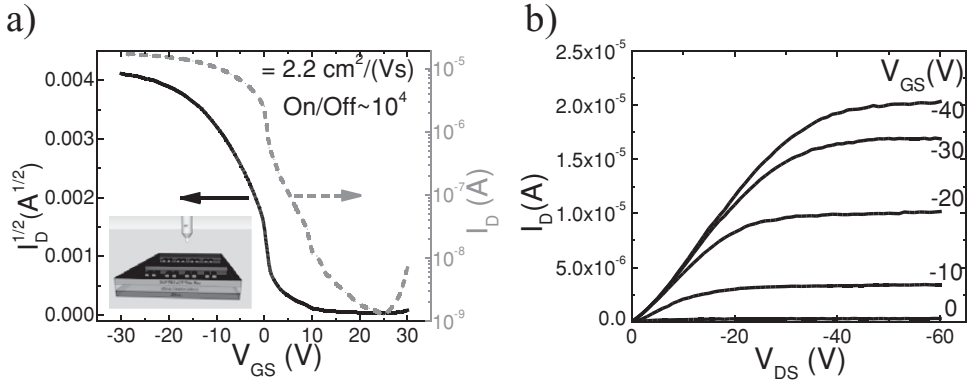

Figure 5. Electronic properties of spray-deposited diF-TEG ADT transistors. a) Transfer characteristics in the saturation regime (V_{DS} = –40 V). Right axis: (log(I_D) vs V_{GS}). Left axis: $\sqrt{I_D}$ vs V_{GS}. b) Output characteristics for the same device.

Adv. Mater. **2013**,
DOI: 10.1002/adma.201205371

3.54 g (77%) of the desired colorless liquid acetylene was isolated.^{1}H NMR (400 MHz, $CDCl_3$) δ: 1.141 (quart, J = 7.3 Hz, 6H), 2.054 (t, J = 7.7 Hz, 9H), 2.533 (s, 1H) ppm.^{13}C NMR (100 MHz, $CDCl_3$) δ: 5.683, 8.923, 8.795, 93.385 ppm. MS (EI 70eV)m/z 182, 184, 185, 186, 188 (2.5:3.5:1:4.5:1, M^+), 153, 155, 156, 157, 159 (2.5:3.5:1:4.5:1, M^+-Et), 125, 127, 128, 129, 131 (2.5:3.5:1:4.5:1, M^+-Et_2+H), 95, 97, 98, 99, 101(2.5:3.5:1:4.5:1, M^+-Et_3).

diF-TEG ADT: Into a flame dried round bottom flask, 2.23 mL (12.5 mmol) triethylgermyl acetylene dissolved in 10 mL of heptane was added. The vessel was cooled to 0 C and 4.38 mL (10.9 mmol) 2.5 M n-BuLi was added. After stirring at room temperature for 1 hour, difluoro ADT quinone (1 g, 3.1 mmol) along with 90 mL heptane and 10 mL dry THF was added and the mixture was stirred at room temperature overnight. After quenching with water the crude diol was dissolved in THF and 2.82 g (12.5 mmol) tin chloride with 100 mL 10% HCl was added. The mixture was allowed to stir at room temperature for 1 hour after which it was extracted with hexane, washed with water, dried, and concentrated. The product was purified using silica column chromatography in hexane to give a dark purple solid. The solid was recrystallized from hexane to give 1.3 g (63%) dark purple crystals.^{1}H NMR (400 MHz, $CDCl_3$) δ: 1.147 (quart, J = 7.81 Hz, 12H); 1.326 (t, J = 7.655 Hz, 18H); 7.430 (d, J = 5.596 Hz, 2 H); 7.520 (d, J = 5.196 Hz, 2H); 9.128 (s, 2H); 9.180 (s, 2H) ppm.^{13}C NMR (100 MHz, $CDCl_3$) δ: 6.421, 9.586, 103.358, 107.662, 120.324, 120.362, 131.600, 121.653, 123.976, 129.768, 129.821, 129.859, 129.904, 130.003, 130.094, 139.431, 139.583, 140.031, 140.129 ppm. MS (MALDI-TOF, no matrix) m/z 650, 652, 654, 656, 658 (2.5:3.5:1:4.5:1, M^+).

Single Crystal X-Ray Diffraction: X-ray data were collected on a Bruker-Nonius X8 Proteum CCD diffractometer using CuK(alpha) radiation. The structures were solved using SHELXS and refined using SHELXL from the SHELX-97 program package.[17] Molecular fragment editing was performed using the XP program of SHELXTL.[17] All non-hydrogen atoms were refined with anisotropic displacement parameters. H atoms were found in difference Fourier maps and subsequently placed in idealized positions within constrained distances of the attached atom. The interplanar distances were determined considering the plane of the three fused 6-membered rings.

Thin-film X-Ray Diffraction: Thin films were fabricated under identical conditions with the SAC FETs (details below). XRD data were collected on a Bruker D8 Discover with DaVinci diffractometer, in the standard Bragg-Brentano para-focusing configuration utilizing sealed tube CuKā radiation and operated at 40 kV and 40 mA. The sample was mounted on a horizontal sample stage on a 830 mm diameter goniometer equipped with a 1D Lynxeye detector. Data were collected using a step width of 0.013 and step time of 0.2 s with a 2θ range of 3.0 - 40.0 . The Bruker Diffrac.Suite Measurement and EVA software packages were used for data collection and processing.[29]

Field-Effect Transistor Fabrication and Characterization: FETs with bottom-gate, bottom-contact configuration were fabricated on highly doped Si gate contact, with a 200 or 300 nm thermally grown SiO_2 gate dielectric and 5 nm Ti/45nm Au source and drain contacts defined by photolithography at channel lengths of 5, 10, 20, 25, 30, 50, 80, and 100 μm, and deposited by e-beam evaporation. These substrates were cleaned in hot acetone, isopropanol, and UV-ozone prior to use. The contacts were treated with PFBT (Sigma Aldrich) by soaking the substrates in a 50 mM room-temperature solution in high purity ethanol (Sigma Aldrich) for 30 minutes followed by sonication in ethanol. In the SAC method for film deposition, a 0.25 wt% solution of the diF-TEG ADT in Chlorobenzene (Sigma Aldrich) was dropped over the substrates and additional solvent was placed around the substrates in a Petri dish with a closed lid to ensure a slow evaporation rate. Spray-deposition was performed from a 0.15 wt% solution in Chlorobenzene using an Iwata Kustom TH K9200 air brush, held at 13 cm above the device substrate, and under 5 psi high purity argon. All devices were placed in a vacuum oven for at least 10 hours to remove possible remaining solvent traces and measured in vacuum using an Agilent 4155C Semiconductor parameter analyzer. Optical micrographs were obtained with an Olympus BH2 UMA microscope, under polarized light.

Fabrication and electrical characterisation of FETs based on polymer/small molecule blends: Top-gate, bottom-contact organic blend transistors were fabricated on glass substrates using Au electrodes treated with PFBT. As-prepared devices had channel lengths and widths varying from 20–100 m and 0.5–2.0 mm respectively. The blend semiconductor was deposited by spin coating at 500 rpm for 10 sec followed by 2000 rpm for 20 sec from 4 wt% 1,2,3,4-tetrahydronaphthalene solutions. The resulting films were annealed at 100 C for 2.5 min to remove excess solvent. Blends consisted of 50:50 by wt% of diF-TEG ADT with poly(triarylamine) (PTAA). The fluoropolymer CYTOP was deposited as the gate dielectric in nitrogen atmosphere followed by the evaporation of the aluminium gate electrode through shadow masks in high vacuum. Electrical characterization was performed in a nitrogen atmosphere using a semiconductor parameter analyzer.

Supporting Information

Supporting Information is available from the Wiley Online Library or from the author.

Acknowledgements

Work at WFU was supported by the National Science Foundation grants ECCS-1102275 and DMR-1040264. Work at U. Kentucky was supported by the Office of Naval Research (N00014-11-1-0329). T.D.A. is grateful to European Research Council (ERC) AMPRO project no. 280221 for financial support.

Received: December 31, 2012
Published online:

[1] a) A. C. Arias, J. D. MacKenzie, I. McCulloch, J. Rivnay, A. Salleo, *Chem. Rev.* **2010**, *110*, 3; b) H. Klauk, *Chem. Soc. Rev.* **2010**, *39*, 2643; c) H. Yan, Z. H. Chen, Y. Zheng, C. Newman, J. R. Quinn, F. Dotz, M. Kastler, A. Facchetti, *Nature* **2009**, *457*, 679; d) T. Sekitani, T. Someya, *Adv. Mater.* **2010**, *22*, 2228; e) S. C. B. Mannsfeld, B. C. K. Tee, R. M. Stoltenberg, C. V. H. H. Chen, S. Barman, B. V. O. Muir, A. N. Sokolov, C. Reese, Z. Bao, *Nat. Mater.* **2010**, *9*, 859.

[2] J. E. Anthony, J. S. Brooks, D. L. Eaton, S. R. Parkin, *J. Am. Chem. Soc.* **2001**, *123*, 9482.

[3] S. Subramanian, S. K. Park, S. R. Parkin, V. Podzorov, T. N. Jackson, J. E. Anthony, *J. Am. Chem. Soc.* **2008**, *130*, 2706.

[4] S. K. Park, D. A. Mourey, S. Subramanian, J. E. Anthony, T. N. Jackson, *Appl. Phys. Lett.* **2008**, *93*, 43301.

[5] O. D. Jurchescu, S. Subramanian, R. J. Kline, S. D. Hudson, J. E. Anthony, T. N. Jackson, D. J. Gundlach, *Chem. Mater.* **2008**, *20*, 6733.

[6] D. Lehnherr, A. R. Waterloo, K. P. Goetz, M. M. Payne, F. Hampel, J. E. Anthony, O. D. Jurchescu, R. R. Tykwinski, *Org. Lett.* **2012**, *14*, 3660.

[7] a) J. L. Bredas, D. Beljonne, V. Coropceanu, J. Cornil, *Chem. Rev.* **2004**, *104*, 4971; b) V. Coropceanu, J. Cornil, D. A. da Silva, Y. Olivier, R. Silbey, J. L. Bredas, *Chem. Rev.* **2007**, *107*, 926.

[8] a) D. J. Gundlach, J. E. Royer, S. K. Park, S. Subramanian, O. D. Jurchescu, B. H. Hamadani, A. J. Moad, R. J. Kline, L. C. Teague, O. Kirillov, C. A. Richter, J. G. Kushmerick, L. J. Richter, S. R. Parkin, T. N. Jackson, J. E. Anthony, *Nat. Mater.* **2008**, *7*, 216; b) J. W. Ward, M. A. Loth, R. J. Kline, M. Coll, C. Ocal, J. E. Anthony, O. D. Jurchescu, *J. Mater. Chem.* **2012**, *22*, 19047; c) R. Li, J. W. Ward, D.-M. Smilgies, M. M. Payne, J. E. Anthony, O. D. Jurchescu, A. Amassian, *Adv. Mater.* **2012**, *24*, 5553.

[9] R. J. Kline, S. D. Hudson, X. R. Zhang, D. J. Gundlach, A. J. Moad, O. D. Jurchescu, T. N. Jackson, S. Subramanian, J. E. Anthony, M. F. Toney, L. J. Richter, *Chem. Mater.* **2011**, *23*, 1194.
[10] K. P. Goetz, Z. Li, J. W. Ward, C. Bougher, J. Rivnay, J. Smith, B. R. Conrad, S. R. Parkin, T. D. Anthopoulos, A. Salleo, J. E. Anthony, O. D. Jurchescu, *Adv. Mater.* **2011**, *23*, 3698.
[11] a) D. J. Gundlach, L. Zhou, J. A. Nichols, T. N. Jackson, P. V. Necliudov, M. S. Shur, *J. Appl. Phys.* **2006**, *100*, 24509; b) B. H. Hamadani, D. Natelson, *J. Appl. Phys.* **2005**, *97*, 64508.
[12] a) E. J. Meijer, C. Detcheverry, P. J. Baesjou, E. van Veenendaal, D. M. de Leeuw, T. M. Klapwijk, *J. Appl. Phys.* **2003**, *93*, 4831; b) X. Guo, R. P. Ortiz, Y. Zheng, Y. Hu, Y.-Y. Noh, K.-J. Baeg, A. Facchetti, T. J. Marks, *J. Am. Chem. Soc.* **2011**, *133*, 1405.
[13] N. Stingelin-Stutzmann, E. Smits, H. Wondergem, C. Tanase, P. Blom, P. Smith, D. De Leeuw, *Nat. Mater.* **2005**, *4*, 601.
[14] a) R. Hamilton, J. Smith, S. Ogier, M. Heeney, J. E. Anthony, I. McCulloch, J. Veres, D. D. C. Bradley, T. D. Anthopoulos, *Adv. Mater.* **2009**, *21*, 1166; b) J. Smith, W. Zhang, R. Sougrat, K. Zhao, R. Li, D. Cha, A. Amassian, M. Heeney, I. McCulloch, T. D. Anthopoulos, *Adv. Mater.* **2012**, *24*, 2441.
[15] C. K. Chan, L. J. Richter, B. Dinardo, C. Jaye, B. R. Conrad, H. W. Ro, D. S. Germack, D. A. Fischer, D. M. DeLongchamp, D. J. Gundlach, *Appl. Phys. Lett.* **2010**, *96*, 133304.
[16] N. A. Azarova, J. W. Owen, C. A. McLellan, M. A. Grimminger, E. K. Chapman, J. E. Anthony O. D. Jurchescu, *Org. Electron.* **2010**, *11*, 1960.
[17] G. M. Sheldrick, *Acta Crystallogr., Sect. A* **2008**, *64*, 112.
[18] L. C. Teague, B. H. Hamadani, O. D. Jurchescu, S. Subramanian, J. E. Anthony, T. N. Jackson, C. A. Richter, D. J. Gundlach, J. G. Kushmerick, *Adv. Mater.* **2008**, *20*, 4513.

Adv. Mater. **2013**,
DOI: 10.1002/adma.201205371